RSC Advances

ROYAL SOCIETY OF CHEMISTRY

www.rsc.org/advances

RSC Advances

ARTICLE

Synthesis of carbazole-based copolymer containing a carbazole-thiazolo[5,4-*d*]thiazole groups with different dopants and their fluorescence, electrical conductivity applications

Received 00th January 20xx,
Accepted 00th January 20xx

DOI: 10.1039/x0xx00000x

www.rsc.org/

Govindasamy Sathiyan[a], Rangasamy Thangamuthu[b] and Pachagounder Sakthivel[a]*

To improve the electrical conductivity of poly(carbazole-thiazolo[5,4-*d*]thiazole) (p-CzTT), five different dopants such as HCl, Fe(III), Cu(II), H_3BO_3, and I_2 were introduced into its framework through protonation of nitrogen atom or complex formation. The carbazole-thiazolo[5,4-d]thiazole (CzTT) and poly(carbazole-thiazolo[5,4-*d*]thiazole) (p-CzTT) were synthesized by the reactions of carbazole aldehydes and dithiooxamide. The synthesized monomer and polymer were confirmed by FT-IR, UV–vis, ^{1}H, ^{13}C-NMR, and GPC studies. The doped polymers were examined by FT-IR spectroscopy, UV–visible absorption, fluorescence, thermogravimetric analysis (TGA), cyclic voltammetry (CV) and electrical conductivity. The optical band gap (E_g^{opt}) of CzTT and p-CzTT were found to be 2.74 eV and 1.95 eV, respectively. The thermal stability of polymer showed 5% weight loss at 358 °C. Based on CV analysis, the HOMO, LUMO energy level and electrochemical band gap (E_g^{cv}) of p-CzTT were obtained as -5.86 eV, -3.19 eV and 2.67 eV, respectively. The CzTT and p-CzTT have exhibited fluorescence emission at 461 nm and 448 nm. Among these dopants, Fe (III) and I_2 doped polymer showed excellent electrical conductivity of 6.8×10^{-5} S cm^{-1} and 5.9×10^{-5} S cm^{-1}, respectively.

1. Introduction

Conducting polymers play a vital role in the conversion of light energy into electrical energy (solar cell) and energy storage devices (battery, supercapacitor, and electrical double layer capacitor).[1,2] Electric devices consist of organic materials which absorption of sunlight and converts photon into electrons (solar cell) and liquid electrolyte reactions (power tools).[3-5] In particular series of organic electronic devices, the conjugated polymers exhibit the presence of π-electrons delocalized as the carriers for an electron moving, character expressed. It has been found that polythiophene, polyacetylene, polyaniline, polypyrrole, and polyphenylene polymers cover a portion of conducting polymers.[6-8]

Over the past few years, π-conjugated fused ring systems have attracted the attention of researcher due to their potential usage in the areas of optics, electronics, and solar energy technologies.[9] The carbazole is a tricyclic fused ring system contains a single nitrogen atom which increases the electron rich nature and hole transporting property.[10] The carbazole-based polymer and small molecules have been considered as a motivating organic semiconductor. The carbazole derivatives have deep-lying highest occupied molecular orbital (HOMO) energy level that is attributed to high open-circuit voltage (V_{oc}). Further, it has high hole mobility due to more preferential π-π stacking that can enhance short-circuit current density (J_{sc}) and fill factor (FF) of the device. Other than conducting properties, the carbazole-based polymers have fluorescence, electro-optical, and hole-transporting properties.[11-15] Nowadays designing of a donor–acceptor (D–A) type molecules was found to be crucial due to their effective photoinduced intramolecular charge-transfer characteristics between donor and acceptor moiety. The thiazolo[5,4-*d*]thiazole (TTz) moiety is commonly employed as acceptor in the system of donor-acceptor (D-A) type polymers owing to their good electron withdrawing properties, planar structures, and easy synthesis.[16] This TTz moiety has a rigid coplanar ring and thereby facilitates intermolecular ordering with high charge-carrier mobility.[17-19] Therefore, introduction of thiazolo[5,4-*d*]thiazole moiety into electron poor alternating copolymers may generate efficient photovoltaic materials with both low band gap and high charge-carrier mobility.[20,21] The structural rigidity of TTz unit in fused with coplanar ring shows low solubility in organic solvents. The solubility of polymer can be increased by introducing alkyl side chain in the π-conjugated fused ring system. Hence, polymers have a fused coplanar as the main backbone with good planarity for intermolecular packing and high charge mobility.[22,23] Olgun et al., have reported a series of copolymer dye of thiazolo[5,4-*d*]thiazolo acceptor moiety and different benzene, triphenylamine as the donor units.[24-28] They have described TTz acceptor moiety-

[a] *Department of Chemistry, School of Advanced Sciences, VIT University, Vellore, Tamil Nadu, India-632 014.*
[b] *Electrochemical Materials Science Division, CSIR-Central Electrochemical Research Institute, Karaikudi-630 003.*
† *Corresponding author. E-mail: sakthivel.p@vit.ac.in and polysathi@gmail.com*

Electronic Supplementary Information (ESI) available: [details of any supplementary information available should be included here]. See DOI: 10.1039/x0xx00000x

containing polymer showed low band gap of 1.36 eV and 2.50 eV. The polymer and their doped polymers exhibit a maximum electrical conductivity of 0.35 μS cm^{-1}. The phenylene and thiazolo[5,4-*d*]thiazoles containing compounds have been investigated for fluorescence, electrical conductivity, and solar cell applications. Previous reports reveal that molecules of poly(phenylene-thiazolo[5,4-*d*]thiazole)[26], thiophene-thiazolo[5,4-d]thiazole,[29] dithiophene-co-thiazolo[5,4-d]thiazole,[30] and poly[{4,4-bis(2-ethylhexyl)-4H-cyclopenta[2,1-b:3,4-b']dithiophene-2,6-diyl}-alt-{2,5-di(thiophen-2-yl)thiazolo-[5,4-d]thiazole-5,5'-diyl}],[31] have been used for solar cell and electrical applications.

In this work, carbazole-thiazolo[5,4-*d*]thiazole (CzTT) and poly(carbazole-thiazolo[5,4-*d*]thiazole) (p-CzTT) were synthesized by the reacting 9-hexyl-9H-carbazole-3-carbaldehyde (or) 9-hexyl-9H-carbazole-3,6-dicarbaldehyde with dithiooxamide. The synthesized p-CzTT was doped with HCl, I_2, Cu(II), Fe(III) and H_3BO_3. The monomer (CzTT) and polymer (p-CzTT) were confirmed by ^1H, ^{13}C-NMR, and GPC. Thermal stability of the p-CzTT has been examined by TGA. The doped and undoped forms of p-CzTT polymer were characterized by UV-vis, FT-IR, and electrical conductivity. The HOMO, LUMO energy levels and the band gap of CzTT and p-CzTT were calculated by cyclic voltammetry (CV).

2. Results and discussion

2.1. Synthesis and doping of p-CzTT polymer

The compounds carbazole-thiazolo[5,4-d]thiazole and poly(carbazole-thiazolo[5,4-*d*]thiazole) (p-CzTT) were synthesized from 9-hexyl-9H-carbazole-3-carbaldehyde, 9-hexyl-9H-carbazole-3,6-dicarbaldehyde, and dithiooxamide. The outline of synthetic procedure adopted is shown in Scheme 1. The carbazole was alkylated by using hexyl bromide. The purpose of introducing hexyl chain in carbazole is to reduce steric hindrance, and increase solubility. Further, the carbazole was formylated in 3,6-poisition by Vilsmeier–Haack formylation reaction. The obtained single and double side aldehyde product was treated with dithiooxamide to get monomer (CzTT) and polymer (p-CzTT). The electron rich carbazole moiety act as p-type and the electron deficient thiazolo[5,4-*d*]thiazole act as n-type material. This alternating copolymer has more push-pull property due to the D-A type polymer structure. The p-CzTT polymer was doped with different dopants such as HCl, Fe(III), Cu(II), H_3BO_3 and I_2. The possible interaction of dopants with polymer is either partially oxidation or reduction. These effects may enhance the electrical conductivity and binding with metal to form a complex. This has been studied by using cyclic voltammetry and fluorescence.

The UV-visible absorption spectrum of monomer (CzTT) exhibited three absorption bands at λ_{max} of 284, 326, and 403 nm. Whereas, the polymer (p-CzTT) follow the same pattern at λ_{max} 282, 338, 557 nm. The polymer (p-CzTT) is stable up to 356 °C as interpreted from TGA curve. The p-CzTT shows fluorescence emissions peak at 448 nm with the corresponding excitation at 338 nm. The undoped and doped polymers are examined for HOMO, LUMO energy level and their band gap using CV.

In this present work, the polymer p-CzTT was doped with different dopants like HCl, Fe(III), Cu(II), H_3BO_3, and I_2. All the dopants effectively react with TTz moiety to form either complex or N-substituted bonds without any effects on carbazole moiety. The dopants such as strong and weak acids can protonate nitrogen atoms of TTz moiety by forming N-H bond or nitrogen-boron bonds. Fe(III) and Cu(II) ions show a redox doping behaviour by favouring a complex formation with TTz moiety. Iodine is also one of the redox dopants which may form complex with N and S atoms. The effect of dopants and their spectroscopic results are discussed.

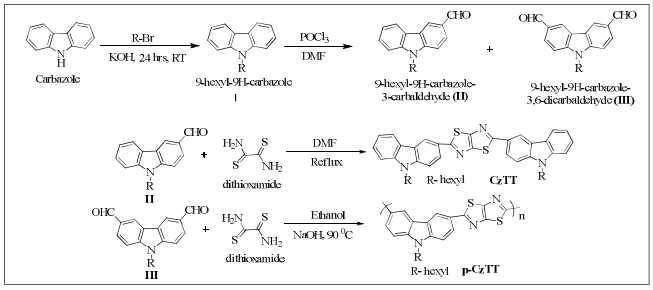

Scheme 1: Synthesis of CzTT and p-CzTT

2.2. GPC molecular weight and Thermal stability

The molecular weight of synthesized polymer was investigated by GPC measurements in THF solution. From GPC, we obtained weight average molecular weight (M_w) of 2498 g/mol and number average molecular weight (M_n) of 2485 g/mol with n = 8 and 9. Thermal properties of polymer (p-CzTT) was investigated by thermogravimetric analysis (TGA) under nitrogen atmosphere at a heating rate of 10 °C min^{-1} as shown in Fig. 1. TGA curve illustrates that 5% decomposition temperature (T_d) of polymer was found to be 358 °C. The polymer has shown high thermal stability which makes it attractive candidate for electrical and solar cell applications.[34]

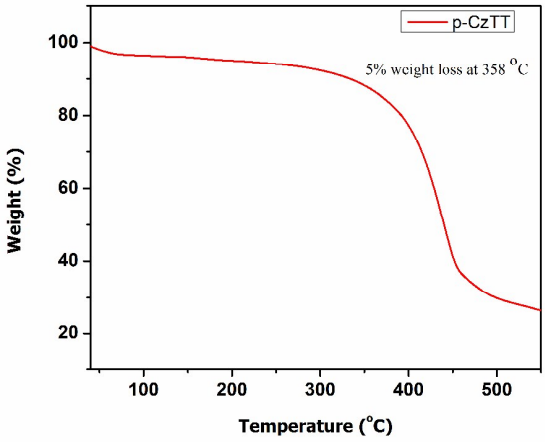

Figure 1. TGA curve of p-CzTT polymer

2.3. ^{1}H-NMR spectroscopy

^{1}H-NMR spectrum of copolymer (p-CzTT) was recorded in DMSO-d_6, and the obtained spectrum is given in Fig. 2. The p-CzTT copolymer containing aldehyde proton (**a**) appeared at 10.13 ppm. The hexyl protons (**c**,**d**,**e**) appears in the range of 0.5-5 ppm whereas the carbazole protons (**b**,*) appears as multiplets in the range 6.5-9.5 ppm. These results confirm the chemical structure of p-CzTT copolymer.

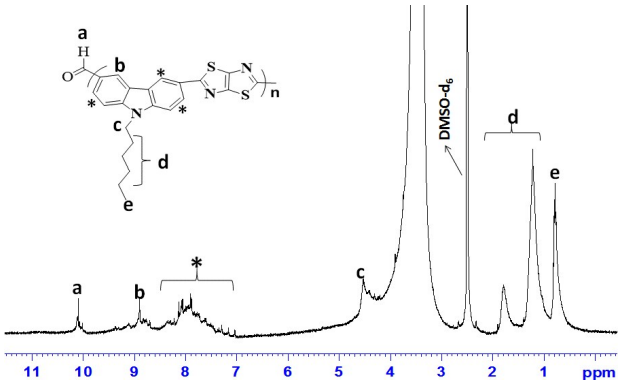

Figure 2. ^{1}H-NMR spectrum of p-CzTT

2.4. FT-IR spectra of undoped and doped polymers

Synthesized and doped polymers were studied by FT-IR spectroscopy. FT-IR spectra recorded by making the solid mixture of polymer with dopants and the obtained spectra are shown in Fig. 3. The obtained results are summarized in Table 1. From FT-IR spectra, effect of various dopants were compared and confirmed the coordination of dopants with polymer. FT-IR spectra of polymer showed the C≡N vibration peak at 1673 cm^{-1} which get shifted to low vibration frequency of 1593 cm^{-1} after HCl addition. This might be due to protonation of nitrogen atoms. The peak at 1192 cm^{-1} indicates B–O vibration of H_3BO_3 doped sample. The shift of peak at 1321 cm^{-1} to 1379 cm^{-1} could be possibly due to bond formation between B–N after doping with H_3BO_3.[25] The characteristic polymer peak at 1321 cm^{-1} completely varied after adding dopant which indicates the formation of new bond between dopant and polymer.[35]

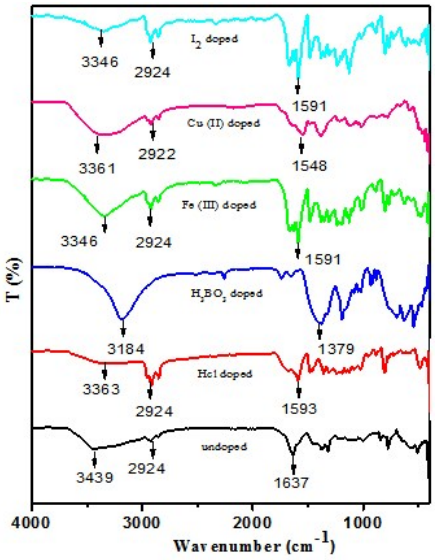

Figure 3. FT-IR spectra of undoped and doped form of polymer samples

Table 1. FT-IR spectra data of undoped and doped polymers.

Samples	FT-IR absorption peak (in cm^{-1})					
p-CzTT	773	-	1321	1637	2924	3439
Cu(II) doped	-	-	1381	1548	2922	3361
Fe(III) doped	804	1236	1483	1591	2924	3346
I_2doped	804	1236	1483	1591	2924	3346
HCl doped	806	1259	1483	1593	2918	3363
H_3BO_3 doped	791	1192	1379	1643	2970	3184

2.5. UV–visible absorption spectroscopy

UV-vis absorption spectra of synthesized monomer (CzTT) and polymer (p-CzTT) were examined in DMF solutions (1.5×10^{-5} M) and absorption results are shown in Fig. 4. CzTT and p-CzTT showed three maximum absorption bands at (284, 282 nm), (326, 338 nm) and (403, 557 nm), respectively. The bands at 326 nm and 338 nm for monomer and polymer indicate the electron transition of π-π* for carbazole moiety. 403 nm and 557 nm bands correspond to thiazolo[5,4-*d*]thiazole (S and N) group for n–σ* electron transition for CzTT and p-CzTT, respectively. Fig. 5 illustrates UV spectra of undoped and HCl doped copolymer in various concentrations. The polymer showed the last band at two shoulder peak λ_{max} wavelength at 524 nm and 557 nm. After, HCl doping the shoulder peak completely shift from 557 nm to 567 nm. This is due to the interaction of HCl proton with polymer nitrogen leading to protonation of N. UV-vis absorbance spectra of Cu(II), Fe(III) and I_2 doped p-CzTT polymer recorded in DMF solvent (0.20 g/L) are shown in Fig. 6. The concentration of dopants are 2N (HCl), 1.81×10^{-4} M (Cu(II)), 1.6×10^{-4} M (Fe(III)), 6.18×10^{-4} M (H_3BO_3) and 1.2×10^{-4} M (I_2) in DMF solutions. The electron withdrawing nature of dopants causes the shift in absorption peaks from lower to higher wavelength. Moreover, it was observed that I_2 doped polymer shows more absorbance compared with other dopants. The monomer and polymer optical band gaps were calculated from UV absorption edge slope and found to be 451, 635 nm, respectively. From these results, the optical band gap for monomer and polymer was found to be 2.74 and 1.95 eV. The doped form of polymer with HCl, Cu(II), Fe(III), H_3BO_3 and I_2 show the optical band gap (E_g^{opt}) of 1.92, 3.17, 2.89, 1.92 and 2.63 eV, respectively. The above mentioned values were calculated from UV absorption edge of 645, 391, 429, 640 and 471 nm, respectively correspond to doped form of polymer with HCl, Cu(II), Fe(III) and I_2.

RSC Advances

ARTICLE

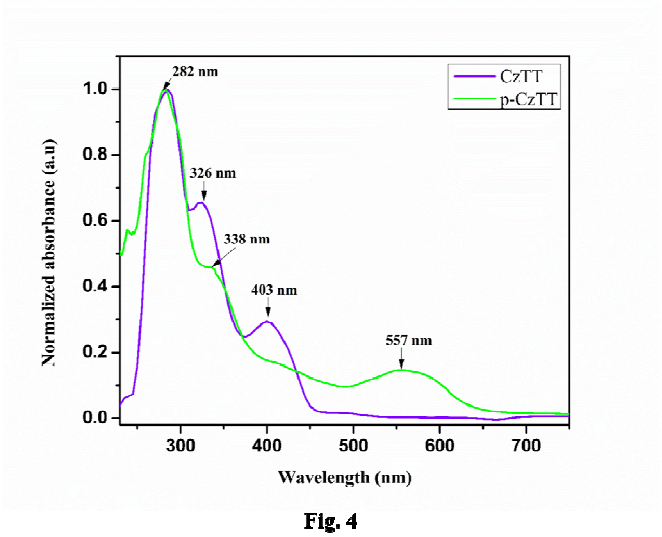

Fig. 4

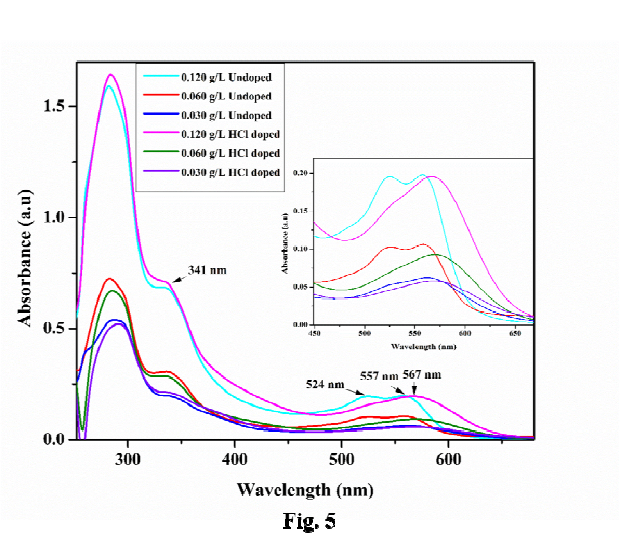

Fig. 5

Figure 4. UV-visible spectra of monomer and polymer in DMF solution; **Figure 5.** UV-visible spectra of polymer and HCl doped polymer for various concentration in DMF solution

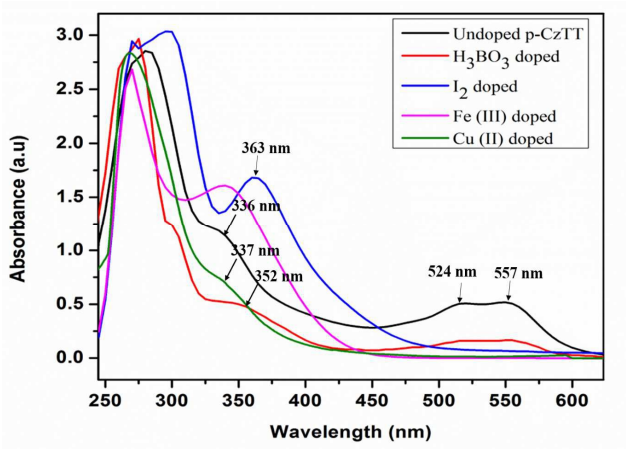

Figure 6. UV-visible spectra of undoped and Fe(III), Cu(II), I_2 doped polymer in DMF solution

2.6. Fluorescence spectroscopy

The synthesized monomer and polymer were characterized by fluorescence (FL) spectroscopy in DMF solvent. The polymer has shown emission peak at 448 nm and excitation peak at 338 nm. The polymer doped with HCl, Cu(II), Fe(III), H_3BO_3 and I_2 has shown the excitation peaks at 341, 341, 340, 342 nm and 363 nm and emission peak at 443, 440, 443, 441 nm and 447 nm, respectively. Further, the FL quantum yields (Φ_F) were measured by using quinine sulfate as the reference standard. The FL quantum yields found to be 0.29 and 0.30 for CzTT and p-CzTT, respectively in DMF solutions. The HCl, Cu(II), Fe(III), H_3BO_3 and I_2 doped polymer shows Φ_F of 0.25, 0.33, 0.36, 0.33 and 0.34, respectively. The Fe (III) and I_2 doped polymers showed more Φ_F value due to the more electron withdrawing nature of the dopant. The undoped polymer quenched with the addition of 0.1 mL HCl increment and fluorescence recorded until completely quenched with an equal molar ratio of polymer and HCl. The fluorescence study was done by 0.1 mL addition of each dopant in the polymer. The FL intensity was observed to be continuously decreasing with the addition of dopant up to equimolar addition. All the emission peaks are almost similar to each other. These results conclude that the dopant-polymer interactions are well identified. The quenching FL intensity and red-shifted emission suggest that polymer molecules have stronger π-π interaction with dopants. The fluorescence results of doped form of polymers reveal intermolecular interaction and enhance the charge carrier transport properties.

RSC Advances

ARTICLE

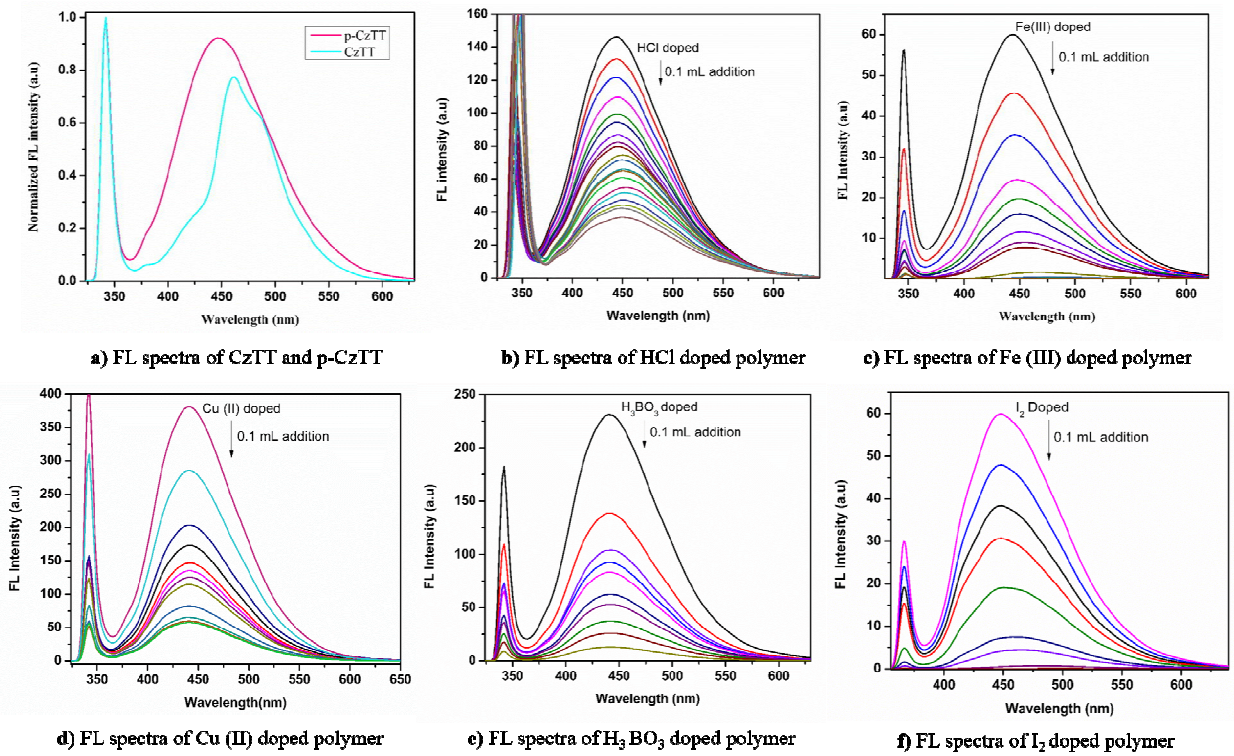

a) FL spectra of CzTT and p-CzTT b) FL spectra of HCl doped polymer c) FL spectra of Fe (III) doped polymer

d) FL spectra of Cu (II) doped polymer e) FL spectra of H_3BO_3 doped polymer f) FL spectra of I_2 doped polymer

Figure 7. Fluorescence spectra of undoped and doped form of polymer

2.7. Electrochemical properties

The electrochemical behaviour of undoped and doped polymer samples was studied by cyclic voltammetry in DMSO solutions with 0.1M $[^{n}Bu_4N]^{+}[PF_6]$ electrolyte solution. The obtained results were shown in Fig. 8, and the data are summarized in Table 2. The onset oxidation potential and reduction onset potential of the undoped polymer were observed at 1.38 eV and -1.29 eV. The HOMO and LUMO energy levels were calculated by using equation 1 and 2. The band gap was calculated from the energy difference between HOMO and LUMO energy levels.

HOMO= -eV (E_{ox}^{onset} - $E_{1/2}$ferrocene + 4.8) . . . . . (1)

LUMO= -eV (E_{red}^{onset} - $E_{1/2}$ferrocene + 4.8) . . . . . (2)

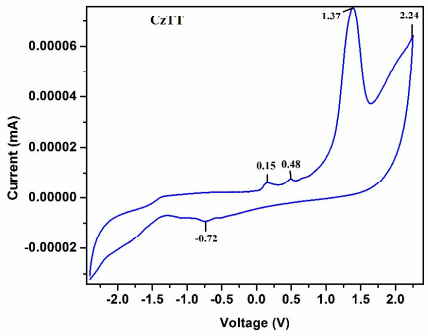

RSC Advances

ARTICLE

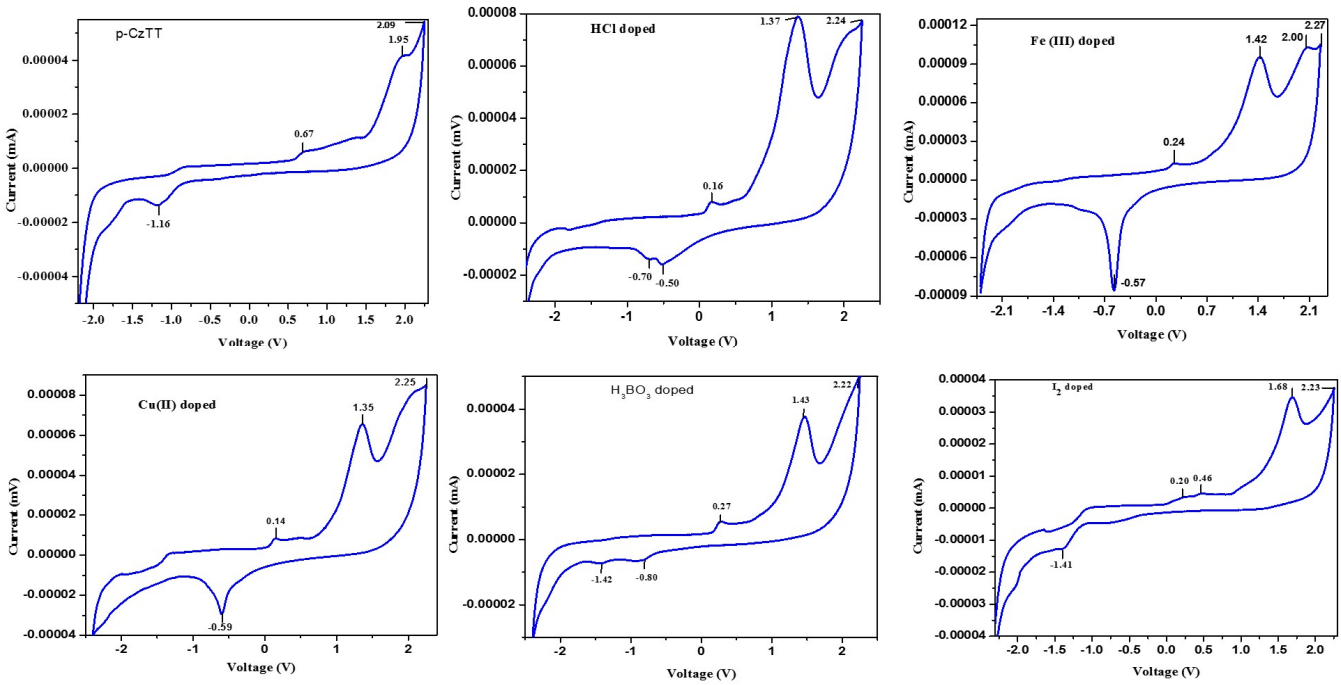

Figure 8. Cyclic voltammograms of undoped and doped form of polymer samples. Scan rate = 100 mV s^{-1}.

Table 2. CV data of undoped and doped polymers.

Samples	Onset oxidation potential (V)	Onset Reduction potential (V)	HOMO (eV)	LUMO (eV)	Band gap (E_g) (eV)
CzTT	0.65	-1.39	-5.11	-3.07	2.04
p-CzTT	1.38	-1.29	-5.86	-3.19	2.67
HCl doped	0.50	-2.02	-4.98	-2.46	2.52
H_3BO_3 doped	0.95	-1.91	-5.43	-3.17	2.26
Cu(II)doped	0.59	-1.40	-5.07	-3.08	1.99
Fe(III)doped	0.54	-1.60	-5.02	-2.88	2.14
I_2 doped	0.82	-0.95	-5.30	-3.53	1.77

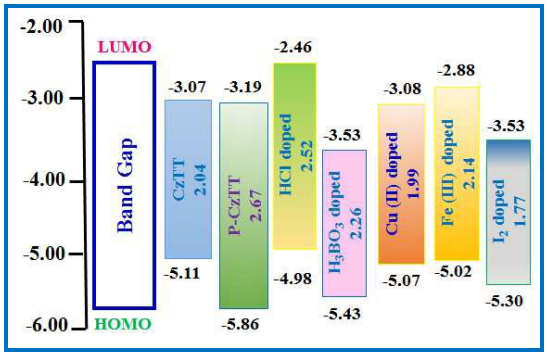

Figure 9. HOMO and LUMO energy level diagram of doped and undoped polymer

In these case of doped polymers enormously changes oxidation and reduction potential due to their ability of oxidation and reduction behaviours. The HOMO, LUMO and the electrochemical band gap of doped and undoped polymer are also given as an energy level diagram in Fig. 9. The metal-doped polymer has shown low band gap compared to acid doped polymer. The Fe(III) doped polymer shows strong reduction potential range at -1.60 eV. The H_3BO_3 and I_2 doped polymer showed deep-lying HOMO energy levels of energy band diagram. CV studies conclude that doped form of polymer can be used in organic photovoltaic applications. Doped forms of polymer showed lowest HOMO and LUMO energy levels compared to undoped polymer. The polymer has shown deep-lying HOMO energy level at -5.86 eV which enhances the open circuit voltage of solar cells whereas the hole mobility and band gap were still low. The doped form of polymer has shown low band gap and lowest HOMO and LUMO energy levels. The H_3BO_3 and I_2 doped polymer showed deep-lying HOMO energy level at -5.43 and -5.30 eV, respectively. The Fe(III) and HCl doped polymer have shown low-lying LUMO energy levels of -2.88 and 2.46 eV, respectively. The Fe(III) and Cu(II) doped polymer show very close HOMO and LUMO energy levels. Wei et al., reported that the ideal polymer showed HOMO, LUMO energy levels and band gap at -5.4 eV, -3.9 eV and 1.5 eV respectively.[36] According to ideal values, our doped form of the polymer sample also showed HOMO and LUMO energy levels close to the reported results due to above reason all these doped forms of the polymer can be used as a donor in bulk heterojunction organic solar cells (BHJ-OSCs) applications.

2.8. SEM microscopy analysis

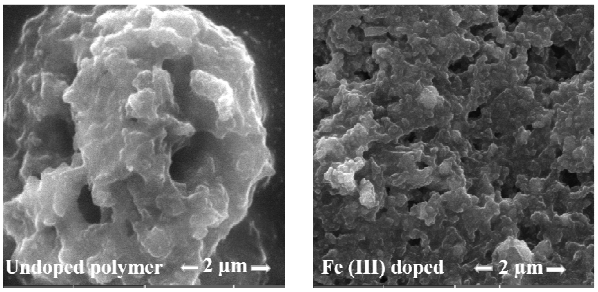

Figure 10. SEM images of undoped and Fe(III) doped polymer

The surface morphology of undoped and Fe(III) doped polymer are investigated by scanning electron microscopy (SEM) analysis and the images are shown in Fig. 10. The surface of undoped p-CzTT sample appears as gel-like morphology. Porus gel network surface covered with tumours was observed for Fe(III) doped polymer. The appearance of tumours might be due to incorporation of Fe(III) in the polymer. Hence, these results indicate that formation of pores might facilitate the electron movement. The incorporation of dopants in polymer promotes easy transportation of electrons leading to the enhanced electric conductivity of doped polymer.

2.9. Powder XRD of doped and undoped polymer

The HCl, Fe(III) doped and undoped polymer samples were studied by powder XRD. XRD patterns (Fig. 11a) shows amorphous nature of undoped polymer used as a precursor. Fig. 11b reveals the presence of multiple elements such as S, HCl, and H. The peaks corresponding to these elements were confirmed by matching with standard JCPDS data card (S: 96-901-2335, 2783; HCl: 96-101-0389 and H: 96-901-3086, 3088), respectively. Thus, it reveals that HCl is successfully doped with the polymer. Similarly, dual peaks were noticed in Fig. 11c. These peaks were found to match with standard JCPDS patterns of Fe (96-900-0667) and S (96-901-2363). These observations prove the presence of Fe(III) in the polymer matrix. The XRD patterns also reveal amorphous nature of polymer samples that can be useful for electrical conductivity applications. HCl doped polymer samples show more crystalline pattern as compared to Fe(III) doped polymer. Due to this crystalline nature of HCl doped polymer shown low electrical conductivity.

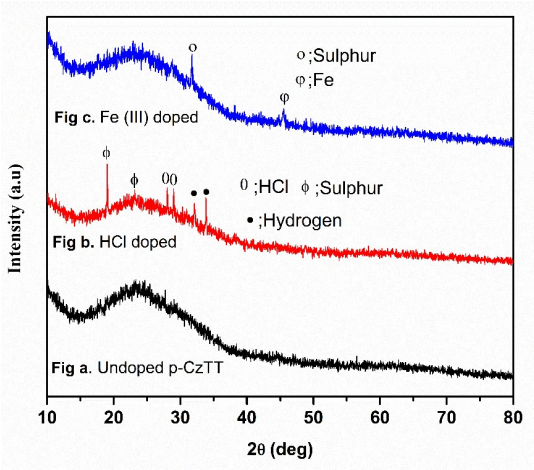

Figure 11. XRD patterns of HCl, Fe(III) doped and undoped polymer

3.0. Electrical conductivity

The electrical conductivity of undoped and doped form of the polymers was measured using impedance spectroscopy method, and the obtained results are shown in Fig. 12. The conductivity was calculated by using equation $\sigma = (L/R_b\ A)$, where, R_b- bulk resistance, L- thickness and A- area of the sample. The conductivity was done at three different temperatures such as 303, 323, 373K and the obtained data are summarized in Table 3. The conductivity of polymer is found to increase with temperature because of enhancement in free volume theory and segmental motion of polymer chain which leads to improving the electrical conductivity of polymer. It is shown in Table 3 that the conductivity values of doped polymer are higher than the undoped polymer with an increase in temperature.[26] This may be due to increasing the overall mobility of electron and free volume of the polymer chains. Since I_2 and Fe(III) are more electron withdrawing group, these dopants may enhance the electrical conductivity. The incorporation of Fe(III) and I_2 dopants can improve the electrical properties in different ways, for example, the porous surface will dissociate the moving of more electron.[34] The HCl doped polymer shown more crystalline nature compare to Fe(III) doped polymer as confirmed by XRD results. The amorphous nature of polymer shows high conductivity as it initiates the breakdown of transient coordination bonds between charge carriers.[35] Due to this, higher electrical conductivity observed in the doped form of the polymers. In the case of 303K, we observed electrical conductivity increases undoped to Fe (III) doped polymers one folds to nine folds. Similarly, the highest temperature 373K the conductivity increase one folds to seven folds. The percentage of the conductivity also increased with respect to the dopant which is shown Table 3. In particularly Fe(III) doped polymer shown maximum electrical conductivity of 6.8×10^{-6} S cm^{-1} at 373 K.

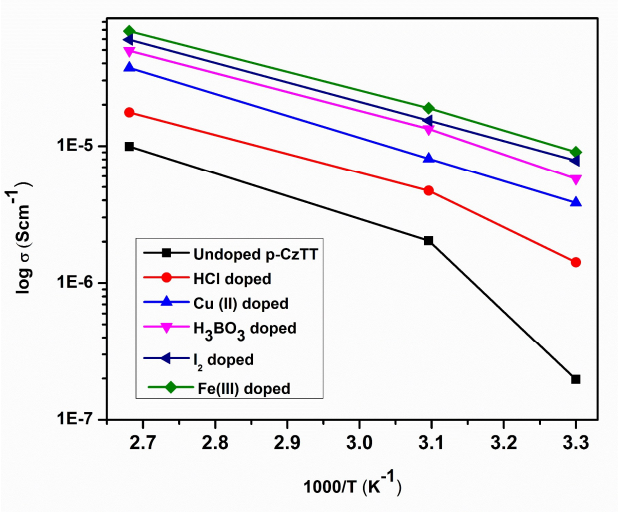

Figure 12. Electrical conductivity of doped and undoped polymer

Table 3. Conductivity values of undoped and doped polymers.

Samples	Conductivity (S cm^{-1})					
	303K	%	323K	%	373K	%
p-CzTT	1.30×10^{-7}	-	1.93×10^{-6}	-	9.89×10^{-6}	-
HCl doped	1.65×10^{-6}	1169	4.68×10^{-6}	143	1.76×10^{-5}	77
Cu(II) doped	3.82×10^{-6}	2838	8.00×10^{-6}	314	3.69×10^{-5}	273
H_3BO_3 doped	5.82×10^{-6}	4376	1.34×10^{-5}	594	4.92×10^{-5}	397
I_2doped	7.81×10^{-6}	5907	1.54×10^{-5}	697	5.93×10^{-5}	499
Fe(III) doped	9.04×10^{-6}	6853	1.90×10^{-5}	884	6.85×10^{-5}	592

4. Conclusions

In conclusion, we observed that addition of dopant to copolymer can have observably decreased in the band gap (E_g^{cv}) and increase the electrical conductivity of p-CzTT. The use of HCl, Cu(II), Fe(III), H_3BO_3 and I_2 dopants has changed their polymer HOMO, LUMO energy levels, optical and electrochemical properties. Also, the polymer exhibits strong FL emission peak at 448 nm and excitation peak at 338 nm range. The Cu(II) and I_2 doped polymers showed very low bang gap of 1.99 and 1.77 eV, respectively. The maximum electrical conductivity had shown that Fe(III) polymer it was found that 6.8×10^{-5} S cm^{-1}. The undoped and doped polymer showed more thermal stability, deep-lying HOMO energy level, and broad

absorption range. This result concluded that doped p-CzTT is a good donor material for BHJ-OSCs applications.

5. Experimental

5.1. Materials

Carbazole, 1-bromohexane, and dithiooxamide were purchased from Sigma-Aldrich Company. Phosphoryl chloride ($POCl_3$), dry dimethylformamide (DMF), dichloromethane (DCM) and chloroform ($CHCl_3$) were obtained from SD Fine-Chem Limited. Dimethyl sulfoxide (DMSO), methanol, HCl solution (37%), $Cu(CH_3COO)_2.H_2O$, $FeCl_3.6H_2O$, H_3BO_3, I_2, Potassium tert-butoxide (t-BuOK), potassium hydroxide (KOH) and sodium hydroxide (NaOH) was purchased from AVRA Company. Other solvents were purchased commercially as AR-grade quality and used without further purification. Column chromatography was performed using silica gel Merck (60-120 mesh).

5.2 Methods

IR Spectra was recorded using SHIMADZU Infrared spectrophotometer (400–4000 cm^{-1}) with resolution IV. The FT-IR spectra were measured by using KBr pellet. ^1H and ^{13}C-NMR spectra were obtained with Bruker 400 MHz spectrometer in $CDCl_3$ and DMSO-d_6 solvent using tetramethylsilane as an internal standard. UV-visible absorption spectra were recorded with a JASCO V-670 spectrophotometer at room temperature. Fluorescence spectra were recorded using Hitachi F-7000FL spectrometer. Thermal analyses were carried out using SDT Q600 V8.3 Build 101 thermogravimetric analyzer (TGA). Cyclic voltammogams were recorded with AutoLab 302 N at a scan rate of 100 mV s^{-1} in 0.1 M solution of tetrabutylammonium tetrafluoroborate in DMSO solution. Two platinum electrodes were used as counter and reference electrode and a glassy carbon electrode as working electrode. Powder XRD was recorded using PANalytical (PW3040/60) at room temperature. The morphology study was carried out using Hitachi (S-3000H) scanning electron microscopy (SEM). The electrical conductivity of the polymer was studied by impedance analysis using 3250 LCR HITESTER meter in the frequency range of 50 Hz to 5 MHz at different temperature (303-373K).

5.2.1. Synthesis of 9-hexyl-9-H-carbazole (I)

Carbazole (3.30 g, 20 mmol), potassium hydroxide (2.96 g, 52.8 mmol) dissolved in DMF (40 mL) and then 1-bromohexane (3.30 g, 20 mmol) was added drop wise. The reaction mixture was stirred at room temperature for 48 h. The reaction mixture was poured into water and extracted with chloroform and dried over anhydrous magnesium sulphate. The solvent was removed by rotary evaporator, the residue was recrystallized in n-hexane to afford compound 1a (4.8 g, 92%) as a white solid. ^1H NMR (400 MHz, $CDCl_3$, ppm): 8.11-8.09 (d, 2H, J=2.4 Hz), 7.46-7.42 (m, 2H), 7.42 -7.39 (d, 2H, J=8.4 Hz), 7.26-7.20 (m, 2H), 4.31-4.28 (t, 2H, J=7.2 Hz), 1.88-1.85 (m, 2H), 1.41-1.37 (m, 6H), 0.86 (t, 3H).

5.2.2. Synthesis of 9-hexyl-9H-carbazole-3-carbaldehyde (II)

$POCl_3$ (25 mL, 0.27 mole) was added drop wise to DMF (35 mL, 0.45 mole) for 30 min at 0 ^oC. Compound 1a (4.00 g, 16 mmol) in dichloromethane (20 mL) was added to the above solution at room temperature after that increase the temperature of 90 ^oC and stirred for 4 h. The reaction mixture was poured into ice-cubes and neutralized with NaOH solution. The solution was extracted three times with ethyl acetate and dried over anhydrous magnesium sulphate. The excess of dichloromethane was removed by vacuum distillation. The crude product was purified by column chromatography (eluent: hexane/ethyl acetate- 9:1) given the product as white colour solid compound (9-hexyl-9H-carbazole-3-carbaldehyde (II), Yield: 68%).^1H NMR ($CDCl_3$, ppm): 10.07 (s, 1H), 8.57 (s, 1H), 8.14-8.12 (d, 1H, J=8 Hz), 8.00- 7.98 (dd, 1H, J=6.8 Hz), 7.55-7.51 (t, 1H, J=8 Hz), 7.44-7.42 (d, 2H, J=8.4 Hz), 7.33-7.30 (t, 1H, J=7.2 Hz), 4.30-4.26 (t, 2H, J=7.6 Hz), 1.90-1.82 (m, 2H), 1.31-1.28 (m, 6H), 0.87 (m, 3H).

5.2.3. Synthesis of 9-hexyl-9H-carbazole-3,6-dicarbaldehyde (III)

$POCl_3$ (25 mL, 0.27 mole) was added drop wise to DMF (35 mL, 0.45 mole) for 1 h at 0 ^oC. Compound 1a (4.00 g, 16 mmol) in dichloromethane (20 mL) was added to the above solution at room temperature after that increase the temperature of 90 ^oC and stirred for 24 h. The same workup procedure has been followed according to the synthesis of compound II. The crude product was purified by column chromatography (eluent: hexane /ethyl acetate- 8:2) using silica gel (2.9 g, Yield: 59%).^1H NMR ($CDCl_3$, ppm): 10.13 (s, 2H), 8.67 (s, 2H), 8.09-8.07 (d, 2H, J=8.4 Hz), 7.56-7.54 (d, 2H, J=8.8 Hz), 4.40-4.36 (t, 2H, J=7.2 Hz), 1.93-1.89 (m, 2H), 1.38-1.34 (m, 6H), 0.86 (m, 3H).

5.2.4. Synthesis of carbazole-thiazolo[5,4-*d*]thiazole (CzTT)

Compound II (0.620 g, 2.2 mmol) and dithiooxamide (0.120 g, 1 mmol) in DMF solution was heated and reflux for 5 hrs under N_2 atm. After the reaction mixture was cooled to room temperature, poured into water extracted with dichloromethane. The organic layer was washed with water and dried over anhydrous magnesium sulphate**.** The crude mixture was purified by column chromatography (eluent: hexane/ethyl acetate- 8:2) given the product as yellow colour solid (yield: 32%). ^1H-NMR ($CDCl_3$, ppm): 8.75 (s, 2H), 8.21-8.19 (d, 2H, J=7.6 Hz), 8.13-8.10 (dd, 2H, J=6.8 Hz), 7.53-7.50 (t, 2H, J=7.2 Hz), 7.48-7.54 (dd-4H, J=4 Hz), 7.24-7.22 (t, 2H, J=2.4 Hz) 4.35-4.32 (t, 4H, J=7.2 Hz), 1.92-1.89 (m, 4H), 1.32-1.25 (m, 12H), 0.89 (m, 6H). ^{13}C-NMR ($CDCl_3$, ppm): 142.06, 141.34, 126.63, 125.59, 124.60, 123.61, 121.07, 119.90, 118.97, 109.37, 43.60, 31.80, 29.94, 27.21, 22.78, and 14.24.

5.2.5. Synthesis of poly(carbazole-thiazolo[5,4-*d*]thiazole) (p-CzTT)

The compound III (0.61 g, 2 mmol) and dithiooxamide (0.20 g, 2 mmol) was mixed with ethanol and stirred at room temperature under N_2 atm. After that, 1 M sodium hydroxide solution was added to the reaction mixture. Then, the temperature increased to 90 °C and stirred overnight, after that reaction mixture cooled to room temperature and poured into methanol. The obtained

precipitate was filtered, washed with cold methanol and dried in an oven at overnight. The compound was further purified by column chromatography (eluent: chloroform) using silica gel and precipitated with ethanol to give the product as a brown colour solid (yield: 68%). The compound p-CzTT was confirmed by ^{1}H-NMR spectroscopy it was shown in Fig. 2.

5.2.5. p-CzTT polymer doped with different dopants

The p-CzTT polymer was doped with HCl, H_3BO_3, Cu(II), Fe(III), and I_2 using $Cu(CH_3\ COO)_2.H_2O$, $FeCl_3.6H_2O$, H_3BO_3 and I_2 chemical agents. The polymer and doped polymers have been recorded by using FT-IR, UV-vis absorption, cyclic voltammetry (CV) and electrical conductivity. The UV-visible spectrometer was performed with the polymer in DMF solution. The cyclic voltammetry measurements, FT-IR and electrical conductivity measurements, the doping processes were carried out by mixing and grinding in the solid phase. 15 mg of solid dopants of $Cu(CH_3COO)_2\ .H_2O$, $FeCl_3\ .6H_2O$, H_3BO_3, and I_2 were added into the each 50 mg of the p-CzTT copolymer.

Acknowledgments

This work was supported by VIT University for providing laboratory facilities. The financial support by DST funded research project board SERB-SB/FT/CS-185/2011.

References

1. V. Malytskyi, J. Simon, L. Patrone, and J. Raimundo, *RSC Adv.,* 2015, 5, 354.
2. R.S. Kularatne, H.D. Magurudeniya, P. Sista, M.C. Biewer and M.C. Stefan, *J. Polym. Sci., Part A: Polym. Chem.,* 2013, 51, 743.
3. J. Delgado, P. Bouit, S. Filippone, M.A. Herranz, and N. Martín, *Chem. Commun.,* 2010, 46, 4853.
4. G. Zhang,Y. Fu, Q. Zhang, and Z. Xie, *Chem. Commun.,* 2010, 46, 4997.
5. Y. Lin, Y. Li, and X. Zhan, *Chem. Soc. Rev.,* 2012, 41, 4245.
6. J. Heinze, B.F. Uribe, and S. Ludwigs, *Chem. Rev.,* 2010, 110, 4724.
7. A.F. Diaz, K.K. Kanazawa and G.P. Gardini, *J. Chem. Soc., Chem. Commun*., 1979, 635
8. G. Tourillon, F. Garnier, *J. Electroanal, Chem.,* 1982, 35,173.
9. G. Sathiyan, E.K.T. Sivakumar, R. Ganesamoorthy, R. Thangamuthu, and P. Sakthivel, *Tetrahedron Lett.,* 2016, 57, 243.
10. P. Sakthivel, H.S. Song, N. Chakravarthi, J.W. Lee, Y.S. Gal, S. Hwang, S.H. Jin, *Polym*., 2013, 54, 4883.
11. S. Ramkumar, S. Manoharan and S. Anandan, *Dyes Pigm.,* 2012, 94, 503.
12. M. Irfan, K.D. Belfield and A. Saeed, *RSC Adv.,* 2015, *5*, 48760.
13. W. Liu, S. Ying, Q. Sun, X. Qiu, H. Zhang, S. Xue and W. Yang, *Dyes Pigm.,* 2016, 125, 8.
14. N. Nagarajan, G. Velmurugan, G. Prabhu, P. Venuvanalingam, and R. Renganathan, *J Lumin.,* 2014, 147, 111.
15. D. Patra, D. Sahu, H. Padhy, D. Kekuda, C.W. Chu, and H. C. Lin, *J. Polym. Sci., Part A: Polym. Chem.,* 2010, 48, 5479.
16. Y. Li, *Acc. Chem. Res.,* 2012, 45, 723.
17. P. Dutta, W. Yang, S.H. Eom, and S.H. Lee, *Org. Electron.,* 2012, 13, 273.
18. H. Z. Akpinar, Y. A. Udum, and L. Toppare, *J. Polym. Sci., Part A: Polym. Chem.,* 2013, 51, 3901.
19. W. Zhang, Q. Feng, Z.S. Wang, and G. Zhou, *Chem Asian J.,* 2013, 8, 939.
20. S. Subramaniyan, H. Xin, F.S. Kim, N.M. Murari, B.A.E. Courtright, and S.A. Jenekhe, *Macromolecules.,* 2014, 47, 4199.
21. Q. Shi, H. Fan, Y. Liu, J. Chen, Z. Shuai, W. Hu, Y. Li, and X. Zhan, *J. Polym. Sci., Part A: Polym. Chem., 2011,* 49, 4875.
22. S.K. Lee, J.M. Cho, Y. Goo, W.S. Shin, J.C. Lee, W.H. Lee, N. Kang, H.K. Shim, and S.J. Moon, *Chem. Commun.,* 2011, 47, 1791.
23. P. Sakthivel, K. Kranthiraja, C. Saravanan, K. Gunasekar, H. Kim, W. Shin, J. Jeong, H. Woo, and S. H. Jin, *J. Mater. Chem.,* 2014, 2, 6916.
24. U. Olgun and M. Gulfen, *React. Funct. Polym.,* 2014, 77, 23.
25. U. Olgun and D.M. Kalyon, *Polymer.,* 2005, 46, 9423.
26. U. Olgun and M. Gulfen, *RSC Adv.,* 2014, 4, 25165.
27. U. Olgun and M. Gulfen, *Dyes Pigm.,* 2014, 102, 189.
28. U. Olgun and M. Gulfen, *Dyes Pigm.,* 2013, 99, 1004.
29. I. Osaka, R. Zhang, G. Sauve, D.M. Smilgies, T. Kowalewski and R.D. Mc Cullough, *J. Am. Chem. Soc.,* 2009, 131, 2521.
30. V.Mierloo, S. Hadipour, A. Spijkman, M.J. Vanden brande, N. Ruttens and B. Kesters, *Chem. Mater.,* 2012, 24, 587.
31. S.P. Mishra, A.K. Palai, A. Kumar, R. Srivastava, M.N. Kamalasanan and M. Patri, *Macromol. Chem. Phys.,* 2010, 211, 1890.
32. B. Umamahesh, M. Saravanakumar, T. Manojkumar and K. I. Sathiyanarayanan, *RSC Adv*., 2016, 6, 58549.
33. M.D. Zipper, G.P. Simon, P. Cherry and A.J. Hill, J. Polym. Sci. B Polym. Phys., 1994, 32, 1237.
34. V. Tamilavan, M. Song, S.H. Jin, H.J. Park, U.C. Yoon and M.H. Hyun. *Synth. Met.,* 2012, 162, 1184.
35. S. Rajendran, R. S. Babu and P. Sivakumar, *J. Power Sources*., 2007, 170, 460.
36. H. Zhou, L. Yang, W.You, *Macromolecules.*, 2012, 45, 607.

Graphical abstract

Synthesis of carbazole-based copolymer containing a carbazole- thiazolo[5,4-*d*]thiazole groups with different dopants and their fluorescence, electrical conductivity applications

Govindasamy Sathiyan[a], Rangasamy Thangamuthu[b] and Pachagoundar Sakthivel[a]*